



OPEN ACCESS

EDITED BY

Renjith Thomas,
Mahatma Gandhi University, India

REVIEWED BY

Ernesto Chigo,
Meritorious Autonomous University of
Puebla, Mexico
Jose Luis Cabellos,
Polytechnic University of Tapachula,
Mexico
Slavko Radenković,
University of Kragujevac, Serbia

*CORRESPONDENCE

Kang-Ning Li,
✉ knli@nxu.edu.cn

SPECIALTY SECTION

This article was submitted to Theoretical
and Computational Chemistry,
a section of the journal
Frontiers in Chemistry

RECEIVED 13 January 2023

ACCEPTED 07 February 2023

PUBLISHED 16 February 2023

CITATION

Li L-K, Ma Y-Q, Li K-N, Xie W-L and
Huang B (2023), Structural and electronic
properties of H₂, CO, CH₄, NO, and NH₃
adsorbed onto Al₁₂Si₁₂ nanocages using
density functional theory.
Front. Chem. 11:1143951.
doi: 10.3389/fchem.2023.1143951

COPYRIGHT

© 2023 Li, Ma, Li, Xie and Huang. This is an
open-access article distributed under the
terms of the [Creative Commons
Attribution License \(CC BY\)](https://creativecommons.org/licenses/by/4.0/). The use,
distribution or reproduction in other
forums is permitted, provided the original
author(s) and the copyright owner(s) are
credited and that the original publication
in this journal is cited, in accordance with
accepted academic practice. No use,
distribution or reproduction is permitted
which does not comply with these terms.

Structural and electronic properties of H₂, CO, CH₄, NO, and NH₃ adsorbed onto Al₁₂Si₁₂ nanocages using density functional theory

Liu-Kun Li¹, Yan-Qiu Ma¹, Kang-Ning Li^{1*}, Wen-Li Xie² and Bin Huang³

¹Ningxia Key Laboratory of Intelligent Sensing for the Desert Information, School of Physics and Electronic-Electrical Engineering, Ningxia University, Yinchuan, China, ²Basic Education Department, Guangdong Ocean University, Yangjiang, China, ³Environmental Monitoring Site of Ningxia Ningdong Energy and Chemical Industry Base, Yinchuan, China

In this study, the adsorption of gases (CH₄, CO, H₂, NH₃, and NO) onto Al₁₂Si₁₂ nanocages was theoretically investigated using density functional theory. For each type of gas molecule, two different adsorption sites above the Al and Si atoms on the cluster surface were explored. We performed geometry optimization on both the pure nanocage and nanocages after gas adsorption and calculated their adsorption energies and electronic properties. The geometric structure of the complexes changed slightly following gas adsorption. We show that these adsorption processes were physical ones and observed that NO adsorbed onto Al₁₂Si₁₂ had the strongest adsorption stability. The E_g (energy band gap) value of the Al₁₂Si₁₂ nanocage was 1.38 eV, indicating that it possesses semiconductor properties. The E_g values of the complexes formed after gas adsorption were all lower than that of the pure nanocage, with the NH₃-Si complex showing the greatest decrease in E_g . Additionally, the highest occupied molecular orbital and the lowest unoccupied molecular orbital were analyzed according to Mulliken charge transfer theory. Interaction with various gases was found to remarkably decrease the E_g of the pure nanocage. The electronic properties of the nanocage were strongly affected by interaction with various gases. The E_g value of the complexes decreased due to the electron transfer between the gas molecule and the nanocage. The density of states of the gas adsorption complexes were also analyzed, and the results showed that the E_g of the complexes decreased due to changes in the 3p orbital of the Si atom. This study theoretically devised novel multifunctional nanostructures through the adsorption of various gases onto pure nanocages, and the findings indicate the promise of these structures for use in electronic devices.

KEYWORDS

nanocage, Al₁₂Si₁₂, equilibrium geometries, stability, electronic properties

1 Introduction

Since Kroto et al. (1985) discovered (C₆₀) fullerene, nanomaterials have gradually become a popular research topic due to their unique properties and wide range of applications (Goroff, 1996; Diederich and Gómez-López, 1999; Kataura et al., 2002; Martín, 2006). Instead of using only C to construct fullerenes, researchers have turned

to fullerenes made from other elements, especially elements from group III of the periodic table and the group V elements that are adjacent to C. These fullerenes include $B_{12}N_{12}$, $Al_{12}N_{12}$, $B_{12}P_{12}$, and $Al_{12}P_{12}$ (Beheshtian et al., 2012a; Beheshtian et al., 2012b; Beheshtian et al., 2012c; Rad and Ayub, 2016; Hussain et al., 2020a). In addition, researchers have used elements from groups II and VI to construct similar fullerene structures, such as $Be_{12}O_{12}$, $Mg_{12}O_{12}$, $Ca_{12}O_{12}$, and all-boron fullerene (Kakemam and Peyghan, 2013; Zhai et al., 2014; Rezaei-Sameti and Abdoli, 2020; Ahsan et al., 2021). Other fullerenes are made from transition elements and oxygen element (de Oliveira et al., 2015). Nanocages with the general formula $(XY)_n$, where n is the number of atoms, are more popular among researchers because they are more stable (Strout, 2000). Many types of nanostructures exist, among which inorganic nanostructures have attracted the attention of researchers due to their extremely high stability and asymmetric charge distribution (Dai, 2002; Tasis et al., 2006; Bindhu et al., 2016). The study of fullerene structures is a critical branch of nanotechnology because of their applications in electronic devices, special materials, and environmental processes. Shakerzdeh et al. (2015) studied the properties of alkali metals (Li, Na, and K) interacting with $Be_{12}O_{12}$ and $Mg_{12}O_{12}$ nanoclusters. Doping with alkali metals can significantly improve the non-linear optical response of nanocages. Beheshtian et al. (2012c) have studied the adsorption of NO and CO by $Al_{12}N_{12}$. Due to the different changes in the E_g (energy band gap) of NO and CO when adsorbed, resulting in different changes in electrical conductivity, $Al_{12}N_{12}$ clusters may selectively detect NO molecules when CO molecules are present. Vergara-Reyes et al. (2021) studied the adsorption of NO on the $C_{36}N_{24}$ fullerene, providing a possible carrier/protector of nitric oxide and thus fulfill its correct biological functions. Escobedo et al. (2019) conducted the effect of chemical order on the structural and physicochemical properties of $B_{12}N_{12}$ fullerene. Bautista Hernandez et al. (2022) found that the $(TiO_2)_{19}$ cluster is a good candidate for storing various gases, and can also be used as a hydrogen storage device.

For China in particular and the rest of the world in general, fossil fuel use must be scaled back, and hydrogen, which has the highest calorific value per unit mass of fuels and produces only water during combustion, is an attractive alternative (Yilanci et al., 2009; Züttel et al., 2010; Mazloomi and Gomes, 2012). Technologies for capturing pollutants and greenhouse gases from the atmosphere will also play a key role in our fight against climate change (Cazorla-Amorós et al., 1996; Zhang et al., 2008; Mastalerz et al., 2011).

Oku et al. (2004) synthesized the first inorganic nanocages in 2004 before the later emergence of $B_{12}N_{12}$, $Al_{12}N_{12}$, $B_{12}P_{12}$, and $Al_{12}P_{12}$ nanocages. Yarovsky and Goldberg, (2005) studied the adsorption of H_2 by Al_{13} clusters using DFT (density functional theory). Thereafter, Felício-Sousa et al. (2021) examined the adsorption properties of H_2 , CO, CH_4 , and CH_3OH on Fe_{13} , Co_{12} , Ni_{13} , and Cu_{13} clusters using an *ab initio* investigation. Tan et al. (2022) studied clusters of different numbers of Al atoms. Yang et al. (2018) predicted the properties of electron redundant Si_nN_n fullerenes. Metal oxide nanocages are also a popular area of research; Otaibi et al. conducted a theoretical study on the adsorption of glycoluril by $Mg_{12}O_{12}$ nanocages (Al-

Otaibi et al., 2022). Some nanocages exhibit unique electronic properties after doping with alkali metals, and these have also been widely studied (Ahsin and Ayub, 2021). We replaced the N atoms in $Al_{12}N_{12}$ with Si atoms to investigate a more diverse range of materials than those in the literature. In this study, we adopted DFT to analyze the properties of $Al_{12}Si_{12}$, such as its stability, after the adsorption of CH_4 , CO, H_2 , NO, and NH_3 .

2 Computational methodology

An $Al_{12}Si_{12}$ nanocage was selected as the model adsorbent. Geometry optimization was performed using hybrid functional DFT (B3LYP) (Becke, 1993) implemented in Gaussian 09 (Frisch et al., 2004). B3LYP is a suitable and widely accepted functional for nanoclusters (Chen et al., 2009; Hussain et al., 2020b). The mixed basis set 6-31G (d, p) was used. Gas molecules CH_4 , CO, H_2 , NO, and NH_3 were adsorbed onto $Al_{12}Si_{12}$ nanocages using the same method. Two adsorption sites on the $Al_{12}Si_{12}$ nanocage were considered. Vibration frequencies were also calculated at equivalent levels to verify that all stationary points corresponded to true minima on the potential energy surface. Geometry optimization was conducted, and D_{ads} (distance of adsorption), E_{ads} (adsorption energy), E_{HOMO} (energy of the highest occupied molecular orbital), E_{LUMO} (energy of lowest unoccupied molecular orbital), DOS (density of states), and Q_T (Mulliken charge transfer) were calculated to determine the adsorption mechanism.

The stability of the $Al_{12}Si_{12}$ nanocage was examined in terms of E_{coh} (cohesive energy), which can be determined by calculating the average energy difference of each atom before and after bonding using the following equation:

$$E_{coh} = \frac{E_{total} - 12(E_{Al} + E_{Si})}{24}$$

where E_{Al} and E_{Si} are the energies of non-interacting Al and Si atoms, respectively, and E_{total} is the energy of the $Al_{12}Si_{12}$ nanocage.

E_{ads} is defined as follows:

$$E_{ads} = E_{adsorbate@nanocage} - E_{adsorbate} - E_{nanocage}$$

Here, $E_{adsorbate@nanocage}$, $E_{adsorbate}$, and $E_{nanocage}$ are the total energies of an adsorbate adsorbed onto the pure nanocage, of the adsorbate, and of the pure nanocage, respectively. A negative value of E_{ads} corresponds to exothermic adsorption. The more negative the adsorption value, the stronger the adsorption capacity. The DOS was generated in Multiwfn (O'Boyle et al., 2008).

3 Results and discussion

3.1 Geometrical characteristics

3.1.1 $Al_{12}Si_{12}$ structure

The optimized structures of the bare nanocage comprising eight hexagons and six tetragon rings are given in Figure 1. In this nanocage, two non-equivalent bonds exist: one between the tetragon and hexagon ring, and the other between the two hexagonal rings, represented as b_{64} and b_{66} , respectively. The

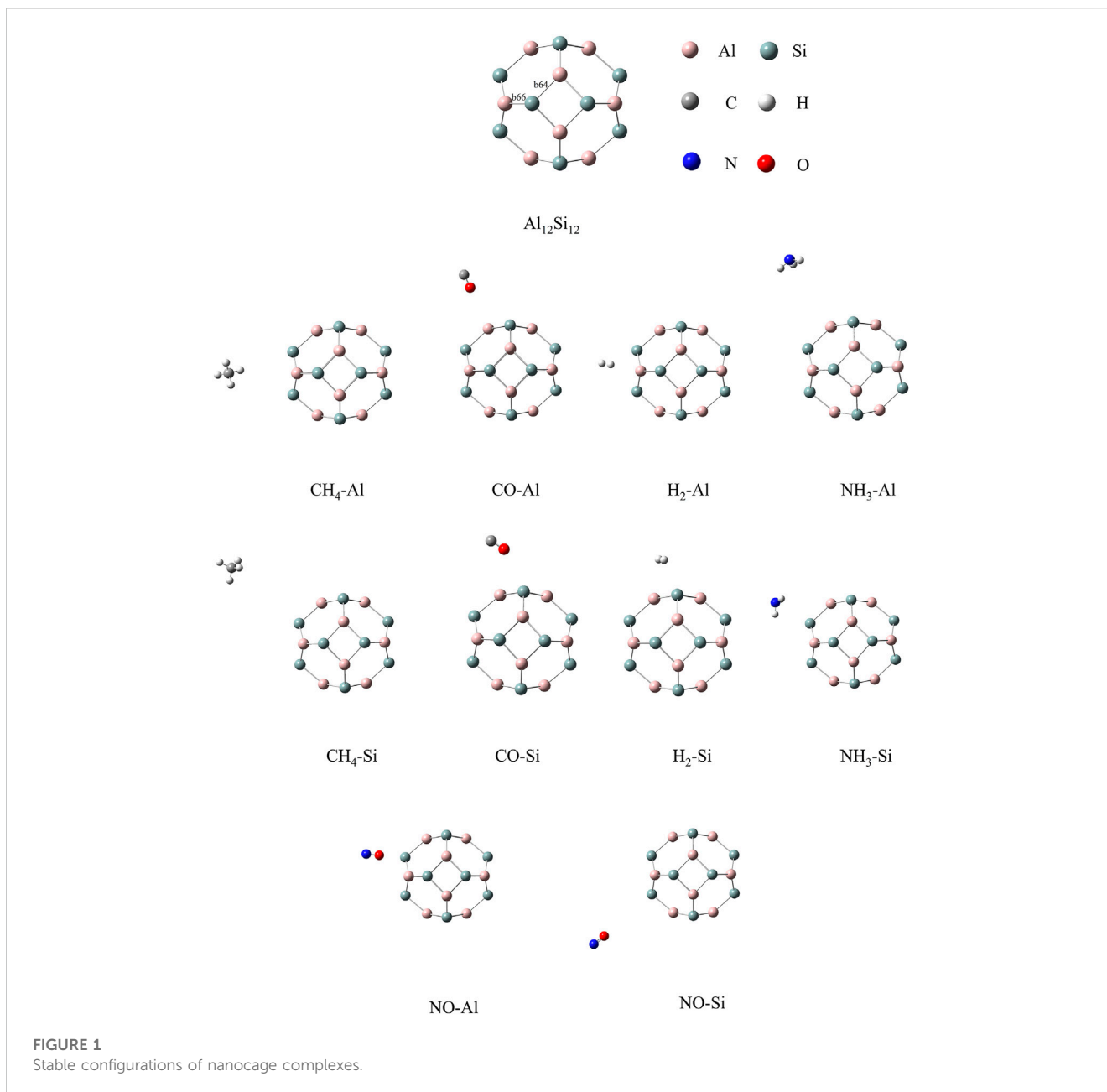
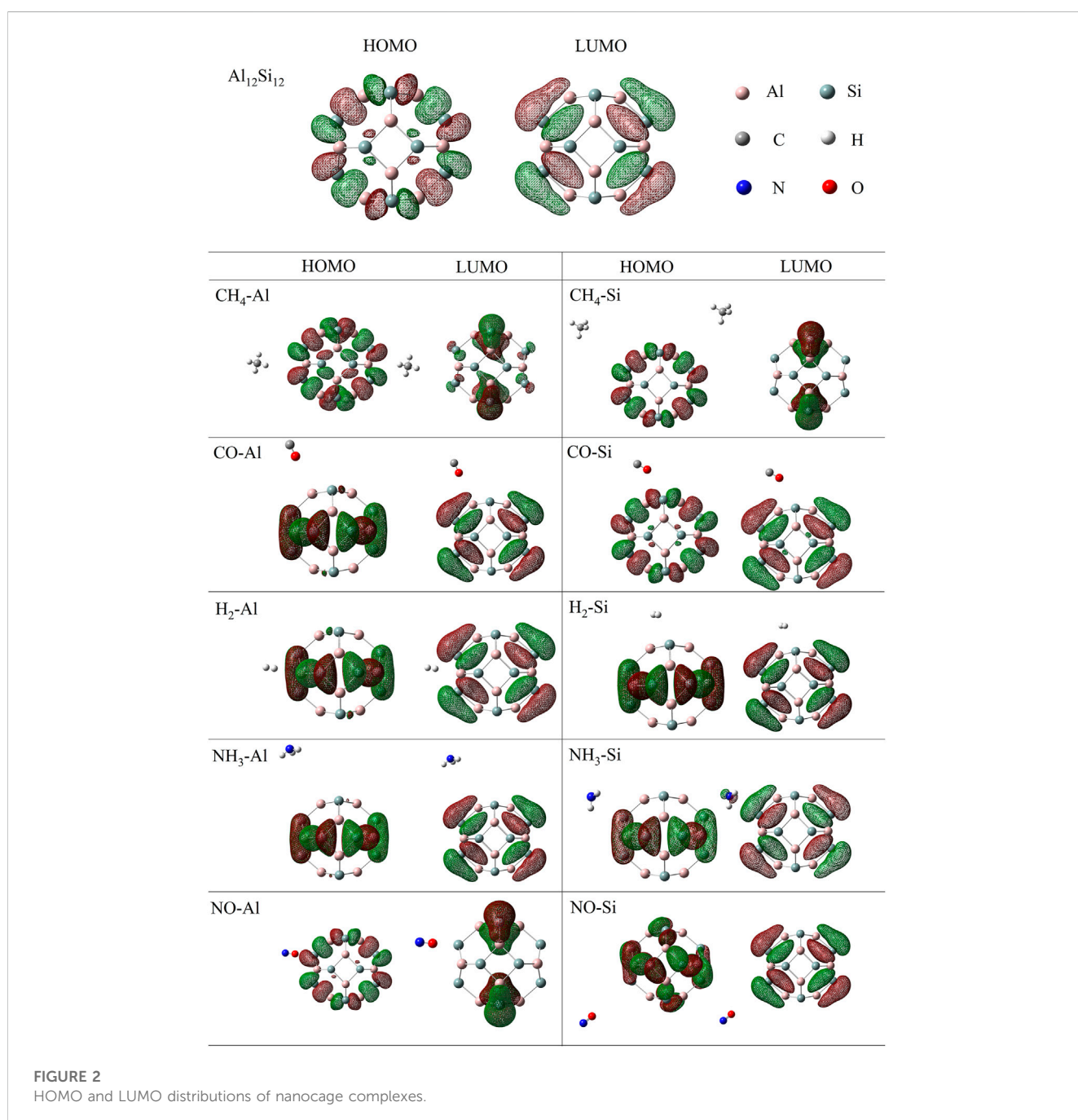


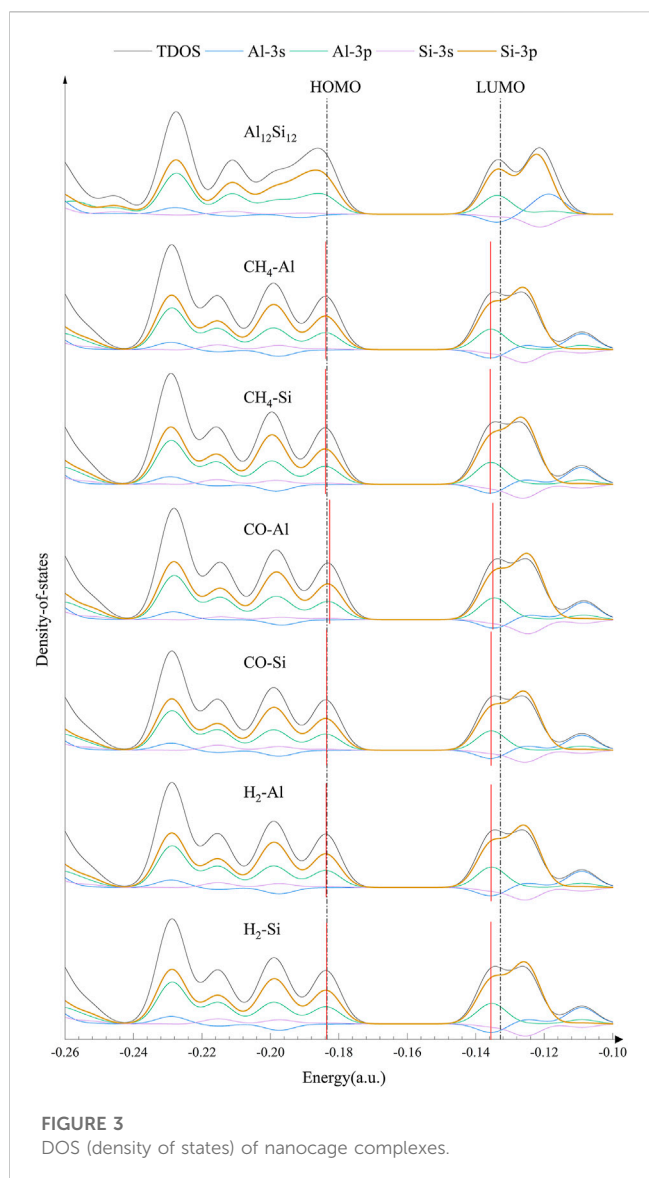
TABLE 1 Bond length (b_{66} and b_{64}), distance of adsorption (D_{ads}) and energy of adsorption (E_{ads}).

| Complexes | b_{66} (Å) | b_{64} (Å) | D_{ads} (Å) | E_{ads} (kcal/mol) | Complexes | b_{66} (Å) | b_{64} (Å) | D_{ads} (Å) | E_{ads} (kcal/mol) |
|--------------------------------|--------------|--------------|----------------------|-----------------------------|--------------------------------|--------------|--------------|----------------------|-----------------------------|
| $\text{Al}_{12}\text{Si}_{12}$ | 2.43 | 2.47 | — | — | $\text{Al}_{12}\text{Si}_{12}$ | 2.43 | 2.47 | — | — |
| $\text{CH}_4\text{-Al}$ | 2.47 | 2.43 | 5.76 | -1.00 | $\text{CH}_4\text{-Si}$ | 2.47 | 2.43 | 7.36 | -1.02 |
| CO-Al | 2.47 | 2.43 | 4.51 | -1.05 | CO-Si | 2.47 | 2.43 | 4.39 | -0.96 |
| $\text{H}_2\text{-Al}$ | 2.47 | 2.43 | 4.52 | -12.37 | $\text{H}_2\text{-Si}$ | 2.47 | 2.43 | 3.92 | -12.34 |
| NO-Al | 2.47 | 2.43 | 3.94 | -15.35 | NO-Si | 2.47 | 2.43 | 5.58 | -15.18 |
| $\text{NH}_3\text{-Al}$ | 2.47 | 2.43 | 6.11 | -0.55 | $\text{NH}_3\text{-Si}$ | 2.47 | 2.42 | 3.48 | -1.23 |

TABLE 2 The Energy of HOMO (E_{HOMO}), energy of LUMO (E_{LUMO}), energy band gap (E_g), change of E_g of nanocage upon the adsorption process (ΔE_g), Mulliken charge transfer (Q_T).

| Complexes | E_{LUMO} (eV) | E_{HOMO} (eV) | E_g (eV) | ΔE_g (eV) | Q_T (e) | Complexes | E_{LUMO} (eV) | E_{HOMO} (eV) | E_g (eV) | ΔE_g (eV) | Q_T (e) |
|-----------------------------------|------------------------|------------------------|------------|-------------------|-------------|-----------------------------------|------------------------|------------------------|------------|-------------------|-------------|
| Al ₁₂ Si ₁₂ | -3.61 | -4.99 | 1.38 | — | — | Al ₁₂ Si ₁₂ | -3.61 | -4.99 | 1.38 | — | — |
| CH ₄ -Al | -3.69 | -5.00 | 1.31 | -0.06 | -0.0022 | CH ₄ -Al | -3.69 | -5.00 | 1.31 | -0.07 | -0.0008 |
| CO-Al | -3.67 | -4.97 | 1.30 | -0.08 | 0.0480 | CO-Al | -3.69 | -5.00 | 1.31 | -0.07 | 0.0001 |
| H ₂ -Al | -3.69 | -4.99 | 1.30 | -0.08 | 0.0197 | H ₂ -Al | -3.69 | -5.00 | 1.31 | -0.07 | 0.0224 |
| NO-Al | -3.70 | -4.99 | 1.29 | -0.09 | 0.0190 | NO-Al | -3.68 | -5.00 | 1.32 | -0.06 | 0.0021 |
| NH ₃ -Al | -3.74 | -5.05 | 1.31 | -0.07 | -0.0021 | NH ₃ -Al | -3.76 | -4.99 | 1.23 | -0.15 | 0.1177 |

**FIGURE 2** HOMO and LUMO distributions of nanocage complexes.



lengths of b_{64} and b_{66} are 2.47 and 2.43 Å, respectively. The calculated E_{coh} of $\text{Al}_{12}\text{Si}_{12}$ is -3.11 eV with zero point energy (ZPE) correction (Buelna-García et al., 2022). The calculated E_{coh} of each atom is closer to the reported E_{coh} of the most stable inorganic analogue, $\text{B}_{12}\text{N}_{12}$. The experimental and theoretical reported E_{coh} of $\text{B}_{12}\text{N}_{12}$ are -4.00 (Pokropivny et al., 2000) and -6.06 eV (Pokropivny and Ovsyannikova, 2007), respectively. As indicated by these results, the $\text{Al}_{12}\text{Si}_{12}$ nanocage is highly stable.

3.1.2 $\text{Al}_{12}\text{Si}_{12}$ –gas molecule structure

CH_4 , CO , H_2 , NO , and NH_3 were selected as the target adsorbates. We performed sufficient structural optimization of the $\text{Al}_{12}\text{Si}_{12}$ nanocage containing CH_4 , CO , H_2 , NO , and NH_3 molecules. For each gas molecule, two different adsorption sites above the Al and Si atoms on the nanocage surface were considered. Each gas is discussed with respect to adsorption at each of the two nanocage positions. The bond length (b_{64} and b_{66}), D_{ads} value (defined as the center to center distance between the atoms of the nanocage and gas molecule that are closest to each other), and

E_{ads} value are listed in Table 1. According to previous studies, the threshold E_{ads} at which physisorption becomes chemisorption is approximately 23.00 kcal/mol (1.00 eV) (Jouypazadeh and Farrokhpour, 2018; Nagarajan and Chandiramouli, 2019; Swetha et al., 2020). D_{ads} must be < 2.00 Å for chemisorption to occur (Contreras et al., 2014). As shown in Table 1, the adsorption processes were all physical, and NO adsorbed above the Al atom of the nanocage had the strongest adsorption stability.

The calculated stable configurations (local minima) are summarized in Figure 1. When the gas was adsorbed onto the Al or Si atom of the $\text{Al}_{12}\text{Si}_{12}$ nanocage, slight local structural deformation of both the molecule and the nanocage occurred. The b_{66} and b_{64} bonds and angles remained almost unchanged. The adsorption that induced greatest change was that of NH_3 onto the Si atom; it changed the lengths of b_{66} and b_{64} by 0.005 and 0.006 Å, respectively. The smallest change was caused by the adsorption of NO onto the Al atom; it changed the lengths of b_{66} and b_{64} by 0.0003 and 0.0204 Å, respectively.

In the Al atom adsorption group, the E_{ads} of CH_4 -Al, CO -Al, NH_3 -Al, NO -Al, and H_2 -Al were -1.00 , -1.05 , -0.55 , -15.35 , and -12.37 kcal/mol, respectively. The adsorption stability of the NO and H_2 analytes was much better than that of the others. The D_{ads} values of NO -Al and H_2 -Al were 3.94 and 4.52 Å, respectively. For NO -Al, the N–O bond length increased from 1.06 Å in isolated NO to 1.16 Å in the adsorbed state. When $\text{Al}_{12}\text{Si}_{12}$ adsorbed H_2 , the H–H bond length increased from 0.6 Å in isolated H_2 to 0.74 Å in the adsorbed state. The D_{ads} between the gas molecule and the Al atom of the nanocage were 5.76 and 4.51 Å for CH_4 -Al and CO -Al, respectively. The C–H bonds of CH_4 -Al and the C–O bond of CO -Al also became slightly longer. The lengths of the four C–H bonds of CH_4 -Al increased by 0.02269, 0.02286, 0.02290, and 0.02313 Å. The length of the C–O bond of CO -Al increased by 0.02 Å. The D_{ads} of NH_3 -Al was 6.11 Å. The length of the three N–H bonds in the NH_3 molecule increased by 0.015636, 0.01599, and 0.01542 Å. Among these complexes, the three N–H bonds of NH_3 -Al had the smallest increase in length.

In the Si atom adsorption group, the E_{ads} of CH_4 -Si, CO -Si, NH_3 -Si, NO -Si, and H_2 -Si were -1.02 , -0.96 , -1.23 , -15.18 , and -12.34 kcal/mol, respectively. The D_{ads} values of CH_4 -Si, CO -Si, NH_3 -Si, NO -Si, and H_2 -Si were 7.36, 4.39, 3.48, 5.58, and 3.92 Å, respectively. In the Si atom adsorption group of complexes, both nanocages and gas molecules changed slightly. The length of the four C–H bonds increased by 0.02253, 0.02268, 0.02284, and 0.02315 Å. The length of the C–O bond increased by 0.02214 Å. The three N–H bonds increased in length by 0.01504, 0.01483, and 0.01485 Å. The lengths of the N–O bond and H–H bond increased by 0.09682, and 0.14372 Å, respectively. Among these complexes, the lengths of the three N–H bonds of NH_3 -Si increased by the least, but they increased by more than those of the three N–H bonds of NH_3 -Al in the Al group.

3.2 Electronic properties

3.2.1 Mulliken charge and energy band gap analysis

Detailed information including the E_{HOMO} and E_{LUMO} , Q_{T} , and the ΔE_{g} (change in, E_{g} of nanocage upon adsorption) values is listed in Table 2.

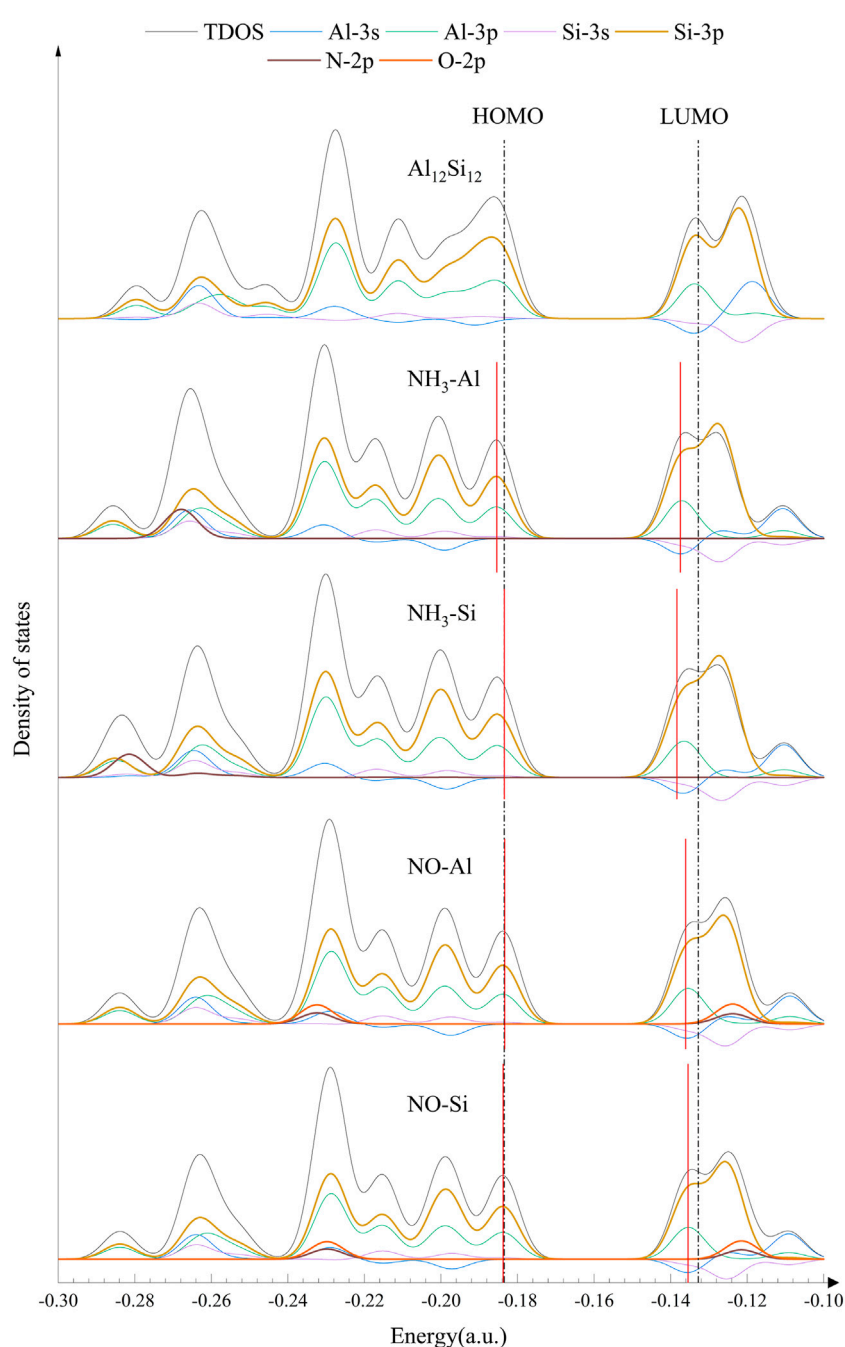


FIGURE 4
DOS (density of states) of nanocage complexes.

In the Al atom adsorption group, the Mulliken charge analysis shows that the number of transferred electrons in CH₄-Al, CO-Al, NH₃-Al, NO-Al, and H₂-Al were -0.0020, -0.0480, -0.0021, 0.0190, and 0.0197 |e|, respectively. The E_g of CH₄-Al, CO-Al, NH₃-Al, NO-Al, and H₂-Al are 1.31, 1.30, 1.31, 1.29, and 1.30 eV, respectively. The E_g of these complexes was lower than that of the pure nanocage, and this decrease was largest in the NO complex, at 0.09 eV, and smallest in the CH₄ complex, at 0.06 eV.

In the Si atom adsorption group, the Mulliken charge analysis demonstrated that the number of transferred electrons in CH₄-Si,

CO-Si, NH₃-Si, NO-Si, and H₂-Si were -0.0008, 0.0001, 0.1177, 0.0021, and 0.0224 |e|, respectively. The E_g of CH₄-Si, CO-Si, NH₃-Si, NO-Si, and H₂-Si was 1.31, 1.31, 1.23, 1.31, and 1.31 eV, respectively. The E_g values of these complexes were also lower than that of the pure nanocage, with the NH₃ complex exhibiting the greatest decrease, at 0.15 eV, and the NO complex exhibiting the smallest decrease at 0.06 eV.

As demonstrated in Table 2, the E_{LUMO} values of these complexes were slightly lower than those of the pure nanocage, but their E_{HOMO} values did not vary much from those of the pure

nanocage. The adsorption stability of the Si adsorption group of complexes is similar to that of the Al adsorption group. However, the adsorbates in the Si adsorption group transferred fewer electrons than the corresponding adsorbates in the Al adsorption group, except for the H₂ and NH₃ analytes. The N atom gained electrons, and the three H atoms lost electrons in the NH₃-Al adsorption. However, the N atom and the three H atoms all lost electrons in the NH₃-Si adsorption due to the difference in adsorption position. The adsorption stability of NH₃-Si was higher than that of NH₃-Al due to the short adsorption distance and the large number of transferred electrons in the NH₃-Si adsorption.

3.2.2 Frontier molecular orbitals and DOS

To further analyze the effect of gas molecules on the electronic properties of nanocages, the HOMO (highest occupied molecular orbital), LUMO (lowest unoccupied molecular orbital) and DOS of isolated and complexed nanocages were analyzed. The HOMO and LUMO distributions of Al₁₂Si₁₂ from a vertical perspective are shown in Figure 2. The HOMO primarily serves as an electron donor, and the LUMO primarily serves as an electron acceptor (Dai, 2002). For the HOMO of the pure Al₁₂Si₁₂ nanocage, the positive and negative areas alternate between Al and Si atoms (in Figure 2 the red area is negative, the green area is positive). However, for the LUMO of the pure Al₁₂Si₁₂ nanocage, the positive and negative areas alternated between the inside and outside of the nanocage and the HOMO and LUMO were distributed on the same plane. The obtained frontier molecular orbital energies (E_{HOMO} and E_{LUMO}) and the calculated, E_g value of the nanocages are shown in Table 2. The E_g of Al₁₂Si₁₂ was approximately 1.38 eV, demonstrating its semiconductor properties.

The HOMO and LUMO plots of the complexes are displayed in Figure 2. The lower the E_g value, the more easily a molecule was excited. In the Al adsorption group, the HOMO and LUMO of complexes were almost unchanged. After gas adsorption, the distribution positions of the HOMO and LUMO changed from being on the same plane to being perpendicular to each other. In the Si adsorption group, the HOMO and LUMO of CO-Si remained on the same plane after adsorption. This may be due to the low number of electron transfers. In NH₃-Si, the LUMO distribution was in the NH₃ molecule. This may be because NH₃-Si has the shortest adsorption distance and the greatest charge transfer. In NO-Si, part of the HOMO is transferred to the quadrilateral ring opposite the top and bottom. This is most likely because the HOMO energy level of NO-Si is lower than that of NO-Al.

For further confirmation of the electronic behavior of these complexes, DOS analyses were performed (shown in Figures 3, 4). The orbitals in the lower energy region of Al₁₂Si₁₂ were mainly the 3p orbitals of the Si and Al atoms. At approximately -0.26 a.u., 3s orbitals of both the Al atoms and the Si atoms were mainly present. The HOMO-LUMO energy level was composed mainly of the 3p orbitals of the Si and Al atoms, whereas the 3s orbitals of Al atoms were also present near the LUMO energy level.

The effect of the gas molecular orbital on the complex orbital when the nanocage adsorbed some gases was not significant (atomic orbitals that do not contribute to the total orbitals are not depicted in Figures 3, 4). We divided the complexes into two groups: The first including gas molecular orbitals that did not contribute to the total orbitals of the complexes, and the second including the gas

molecular orbitals that contributed to the total orbitals of the complexes. In the first group, after gas adsorption, a new peak at 0.2 a.u. appeared, resulting in a slight decrease in the HOMO of the complexes (except for CO-Al). In addition, due to the adsorption of the gas molecule, the 3s orbital of the Al atom produced a small peak at -0.12 a.u. (shown by the blue curve), causing the peak at -0.11 a.u. to shift to the right slightly. This may be the reason for the decrease in LUMO energy level. In the second group, after gas adsorption, a new peak also appeared at 0.2 a.u.. The 3p orbital of the N atom in NH₃-Al peaked at -0.27 a.u., whereas it peaked at -0.28 a.u. in NH₃-Si (depicted by the brown curve). The 3p orbitals of the N and O atoms in NO-Al and NO-Si had peaks at -0.23 and -0.12 a.u. (the brown curve and the orange curve), respectively. Moreover, the peak value of the 3p orbital of the O atom was greater than that of the N atom. However, compared with the first group, the new peaks in the second group caused almost no decrease in HOMO and LUMO energy levels. The peak generated at 0.2 a.u. of the 3p orbital of the Si and Al atoms was the main reason for the reduction in HOMO energy level.

4 Conclusion

DFT calculations were performed to investigate the equilibrium geometries, stabilities, and electronic properties of gases adsorbed onto Al₁₂Si₁₂ nanocages. The E_g value of Al₁₂Si₁₂ was 1.38 eV, demonstrating the semiconductor properties of the nanocage. We performed structural optimization of Al₁₂Si₁₂ nanocages with adsorbed CH₄, CO, H₂, NO, and NH₃ molecules to study their adsorption energies, equilibrium geometry, and electronic properties. Two adsorption positions on the nanocage were studied. The adsorption energy of these complexes demonstrated that the adsorption of these gases by Al₁₂Si₁₂ nanocages is physical. Our findings reveal that the stabilities of the complexes are as follows: Al₁₂Si₁₂-NO > Al₁₂Si₁₂-H₂ > Al₁₂Si₁₂-NH₃ > Al₁₂Si₁₂-CH₄ > Al₁₂Si₁₂-CO. The geometric structure of the nanocage changed slightly following adsorption of molecules. The E_g of the complexes was lower than that of the pure nanocage due to the electron transfer between the gas molecules and the nanocage. The more electrons were transferred, the greater the decrease in E_g . Except for the 3p orbitals of the N and O atoms, the orbitals of the gas molecules did not contribute to the total orbitals of the complexes. The 3p orbitals of the Si atoms in the Al₁₂Si₁₂ nanocage are the main reason for the change in HOMO-LUMO energy levels detected.

Data availability statement

The original contributions presented in the study are included in the article/supplementary material, further inquiries can be directed to the corresponding author.

Author contributions

Conceptualization, L-KL and K-NL; methodology, K-NL; software, W-LX; validation, Y-QM; formal analysis, L-KL; investigation, BH; resources, BH; data curation, K-NL; writing original draft preparation, L-KL; writing—review and editing, K-NL; visualization, W-LX;

supervision, K-NL; project administration, BH; funding acquisition, K-NL. All authors have read and agreed to the published version of the manuscript.

Funding

This work was supported by the National Natural Science Foundation of China, grant number 42167016. The Natural Science Foundation of Ningxia Province in China, grant number 2022AAC03123. The Key Research and Development Program of Ningxia Province in China, grant number 2020BEB04003, and the fifth batch of the Ningxia Youth Science and Technology Talents Project, grant number NXTJGC147.

References

- Ahsan, A., Khan, S., Gilani, M. A., and Ayub, K. (2021). Endohedral metallofullerene electrides of $\text{Ca}_{12}\text{O}_{12}$ with remarkable nonlinear optical response. *RSC Adv.* 11 (3), 1569–1580. doi:10.1039/d0ra08571e
- Ahsin, A., and Ayub, K. (2021). Extremely large static and dynamic nonlinear optical response of small superalkali clusters NM_3M^+ ($\text{M}, \text{M}^+ = \text{Li}, \text{Na}, \text{K}$). *J. Mol. Graph. Model.* 109, 108031. doi:10.1016/j.jmgn.2021.108031
- Al-Otaibi, J. S., Mary, Y. S., Mary, Y. S., Acharjee, N., and Churchill, D. G. (2022). Theoretical study of glycoluril by highly symmetrical magnesium oxide $\text{Mg}_{12}\text{O}_{12}$ nanostructure: Adsorption, detection, SERS enhancement, and electrical conductivity study. *J. Mol. Model.* 28 (10), 332. doi:10.1007/s00894-022-05332-3
- Bautista Hernandez, A., Chigo Anota, E., Severiano Carrillo, F., Vázquez Cuchillo, O., and Salazar Villanueva, M. (2022). *In-silico* study of the adsorption of H_2 , CO and CO_2 chemical species on $(\text{TiO}_2)_n$ $n=15-20$ clusters: The $(\text{TiO}_2)_{19}$ case as candidate promising. *J. Mol. Graph. Model.* 117, 108316. doi:10.1016/j.jmgn.2022.108316
- Becke, A. D. (1993). Density-functional thermochemistry. III. The role of exact exchange. *J. Chem. Phys.* 98 (7), 5648–5652. doi:10.1063/1.464913
- Beheshtian, J., Bagheri, Z., Kamfiroozi, M., and Ahmadi, A. (2012). A comparative study on the $\text{B}_{12}\text{N}_{12}$, $\text{Al}_{12}\text{N}_{12}$, $\text{B}_{12}\text{P}_{12}$ and $\text{Al}_{12}\text{P}_{12}$ fullerene-like cages. *J. Mol. Model.* 18 (6), 2653–2658. doi:10.1007/s00894-011-1286-y
- Beheshtian, J., Kamfiroozi, M., Bagheri, Z., and Peyghan, A. A. (2012). $\text{B}_{12}\text{N}_{12}$ Nanocage as potential sensor for NO_2 Detection. *Chin. J. Chem. Phys.* 25 (1), 60–64. doi:10.1088/1674-0068/25/01/60-64
- Beheshtian, J., Peyghan, A. A., and Bagheri, Z. (2012). Selective function of $\text{Al}_{12}\text{N}_{12}$ nano-cage towards NO and CO molecules. *Comput. Mat. Sci.* 62, 71–74. doi:10.1016/j.commatsci.2012.05.041
- Bindhu, M. R., Umadevi, M., Kavin Micheal, M., Arasu, M. V., and Abdullah Al-Dhabi, N. (2016). Structural, morphological and optical properties of MgO nanoparticles for antibacterial applications. *Mat. Lett.* 166, 19–22. doi:10.1016/j.matlet.2015.12.020
- Buelna-García, C. E., Castillo-Quevedo, C., Quiroz-Castillo, J. M., Paredes-Sotelo, E., Cortez-Valadez, M., Martín-del-Campo-Solis, M. F., et al. (2022). Relative populations and IR spectra of Cu_38 cluster at finite temperature based on DFT and statistical thermodynamics calculations. *Front. Chem.* 10, 841964. doi:10.3389/fchem.2022.841964
- Cazorla-Amorós, D., Alcañiz-Monge, J., and Linares-Solano, A. (1996). Characterization of activated carbon fibers by CO_2 adsorption. *LANGMUIR* 12 (11), 2820–2824. doi:10.1021/la960022s
- Chen, L., Zhou, G.-Q., Xu, C., Zhou, T., and Huo, Y. (2009). Structural and electronic properties of hydrated MgO nanotube clusters. *J. Mol. Struct-Theochem.* 900 (1), 33–36. doi:10.1016/j.theochem.2008.12.019
- Contreras, M. L., Cortés-Arriagada, D., Villarroel, I., Alvarez, J., and Rozas, R. (2014). Evaluating the hydrogen chemisorption and physisorption energies for nitrogen-containing single-walled carbon nanotubes with different chiralities: A density functional theory study. *Struct. Chem.* 25 (4), 1045–1056. doi:10.1007/s11224-013-0377-z
- Dai, H. (2002). Carbon nanotubes: Opportunities and challenges. *Surf. Sci.* 500 (1), 218–241. doi:10.1016/s0039-6028(01)01558-8
- de Oliveira, O. V., Pires, J. M., Neto, A. C., and Divino dos Santos, J. (2015). Computational studies of the $\text{Ca}_{12}\text{O}_{12}$, $\text{Ti}_{12}\text{O}_{12}$, $\text{Fe}_{12}\text{O}_{12}$ and $\text{Zn}_{12}\text{O}_{12}$ nanocage clusters. *Chem. Phys. Lett.* 634, 25–28. doi:10.1016/j.cpl.2015.05.069
- Diederich, F., and Gómez-López, M. (1999). Supramolecular fullerene chemistry. *Chem. Soc. Rev.* 28 (5), 263–277. doi:10.1039/a804248i
- Escobedo, A., Bautista-Hernandez, A., Camacho-García, J. H., Cortes-Arriagada, D., and Chigo-Anota, E. (2019). Effect of chemical order in the structural stability and physicochemical properties of $\text{B}_{12}\text{N}_{12}$ fullerenes. *Sci. Rep.-UK.* 9, 16521. doi:10.1038/s41598-019-52981-1
- Felicio-Sousa, P., Andriani, K. F., and Da Silva, J. L. F. (2021). *Ab initio* investigation of the role of the d-states occupation on the adsorption properties of H_2 , CO , CH_4 and CH_3OH on the Fe_{13} , Co_{13} , Ni_{13} and Cu_{13} clusters. *Phys. Hys. Chem. Chem. Phys.* 23 (14), 8739–8751. doi:10.1039/d0cp06091g
- Frisch, M. J., Trucks, G. W., Schlegel, H. B., Scuseria, G. E., Robb, M. A., Cheeseman, J. R., et al. (2004). *Gaussian 03, revision D.01*. Wallingford, CT: Gaussian, Inc.
- Goroff, N. S. (1996). Mechanism of fullerene formation. *Acc. Chem. Res.* 29 (2), 77–83. doi:10.1021/ar950162d
- Hussain, S., Hussain, R., Mehboob, M. Y., Chatha, S. A. S., Hussain, A. I., Umar, A., et al. (2020). Adsorption of phosgene gas on pristine and copper-decorated $\text{B}_{12}\text{N}_{12}$ nanocages: A comparative DFT study. *ACS Omega* 5 (13), 7641–7650. doi:10.1021/acsomega.0c00507
- Hussain, S., Shahid Chatha, S. A., Hussain, A. I., Hussain, R., Mehboob, M. Y., Gulzar, T., et al. (2020). Designing novel Zn-decorated inorganic $\text{B}_{12}\text{P}_{12}$ nanoclusters with promising electronic properties: A step forward toward efficient CO_2 sensing materials. *ACS Omega* 5 (25), 15547–15556. doi:10.1021/acsomega.0c01686
- Jouypazadeh, H., and Farrokhpour, H. (2018). DFT and TD-DFT study of the adsorption and detection of sulfur mustard chemical warfare agent by the C_{24} , $\text{C}_{12}\text{Si}_{12}$, $\text{Al}_{12}\text{N}_{12}$, $\text{Al}_{12}\text{P}_{12}$, $\text{Be}_{12}\text{O}_{12}$, $\text{B}_{12}\text{N}_{12}$ and $\text{Mg}_{12}\text{O}_{12}$ nanocages. *J. Mol. Struct.* 1164, 227–238. doi:10.1016/j.molstruc.2018.03.051
- Kakemam, J., and Peyghan, A. A. (2013). Electronic, energetic, and structural properties of C- and Si-doped $\text{Mg}_{12}\text{O}_{12}$ nano-cages. *Comput. Mat. Sci.* 79, 352–355. doi:10.1016/j.commatsci.2013.06.036
- Kataura, H., Maniwa, Y., Abe, M., Fujiwara, A., Kodama, T., Kikuchi, K., et al. (2002). Optical properties of fullerene and non-fullerene peapods. *Appl. Phys. A* 74 (3), 349–354. doi:10.1007/s003390201276
- Kroto, H. W., Heath, J. R., O'Brien, S. C., Curl, R. F., and Smalley, R. E. (1985). C_{60} : Buckminsterfullerene. *Nature* 318 (6042), 162–163. doi:10.1038/318162a0
- Martin, N. (2006). New challenges in fullerene chemistry. *Chem. Commun.* (20), 2093–2104. doi:10.1039/b601582b
- Mastalerz, M., Schneider, M. W., Oettel, I. M., and Presley, O. (2011). A salicylbisimine cage compound with high surface area and selective CO_2/CH_4 adsorption. *Angew. Chem. Int. Ed.* 50 (5), 1046–1051. doi:10.1002/anie.201005301
- Mazloomi, K., and Gomes, C. (2012). Hydrogen as an energy carrier: Prospects and challenges. *Renew. Sust. Energy Rev.* 16 (5), 3024–3033. doi:10.1016/j.rser.2012.02.028
- Nagarajan, V., and Chandiramouli, R. (2019). Acrylonitrile vapor adsorption studies on armchair arsenene nanoribbon based on DFT study. *Appl. Surf. Sci.* 494, 1148–1155. doi:10.1016/j.apsusc.2019.07.214
- O'Boyle, N. M., Tenderholt, A. L., and Langner, K. M. (2008). cclib: A library for package-independent computational chemistry algorithms. *J. Comput. Chem.* 29 (5), 839–845. doi:10.1002/jcc.20823
- Oku, T., Nishiwaki, A., and Narita, I. (2004). Formation and atomic structure of $\text{B}_{12}\text{N}_{12}$ nanocage clusters studied by mass spectrometry and cluster calculation. *Sci. Technol. Adv. Mat.* 5 (5), 635–638. doi:10.1016/j.stam.2004.03.017

Conflict of interest

The authors declare that the research was conducted in the absence of any commercial or financial relationships that could be construed as a potential conflict of interest.

Publisher's note

All claims expressed in this article are solely those of the authors and do not necessarily represent those of their affiliated organizations, or those of the publisher, the editors and the reviewers. Any product that may be evaluated in this article, or claim that may be made by its manufacturer, is not guaranteed or endorsed by the publisher.

- Pokropivny, V. V., and Ovsyannikova, L. I. (2007). Electronic structure and the infrared absorption and Raman spectra of the semiconductor clusters C₂₄, B₁₂N₁₂, Si₁₂C₁₂, Zn₁₂O₁₂, and Ga₁₂N₁₂. *Phys. Solid State* 49 (3), 562–570. doi:10.1134/s1063783407030328
- Pokropivny, V. V., Skorokhod, V. V., Oleinik, G. S., Kurdyumov, A. V., Bartnitskaya, T. S., Pokropivny, A. V., et al. (2000). *J. Solid State Chem.* 154 (1), 214.
- Rad, A. S., and Ayub, K. (2016). Ni adsorption on Al₁₂P₁₂ nano-cage: A DFT study. *J. Alloys Compd.* 678, 317–324. doi:10.1016/j.jallcom.2016.03.175
- Rezaei-Sameti, M., and Abdoli, S. K. (2020). The capability of the pristine and (Sc, Ti) doped Be₁₂O₁₂ nanocluster to detect and adsorb of mercaptopyrindine molecule: A first principle study. *J. Mol. Struct.* 1205, 127593. doi:10.1016/j.molstruc.2019.127593
- Shakerzdeh, E., Tahmasebi, E., and Shamlouei, H. R. (2015). The influence of alkali metals (Li, Na and K) interaction with Be₁₂O₁₂ and Mg₁₂O₁₂ nanoclusters on their structural, electronic and nonlinear optical properties: A theoretical study. *Synth. Mater.* 204, 17–24. doi:10.1016/j.synthmet.2015.03.008
- Strout, D. L. (2000). Structure and stability of boron Nitrides: isomers of B₁₂N₁₂. *J. Phys. Chem. A* 104 (15), 3364–3366. doi:10.1021/jp994129a
- Swetha, B., Nagarajan, V., Soltani, A., and Chandiramouli, R. (2020). Novel gamma arsenene nanosheets as sensing medium for vomiting agents: A first-principles research. *Comput. Theor. Chem.* 1185, 112876. doi:10.1016/j.comptc.2020.112876
- Tan, L.-P., Die, D., and Zheng, B.-X. (2022). Growth mechanism, electronic properties and spectra of aluminum clusters. *Spectrochim. Acta. A* 267, 120545. doi:10.1016/j.saa.2021.120545
- Tasis, D., Tagmatarchis, N., Bianco, A., and Prato, M. (2006). Chemistry of carbon nanotubes. *Chem. Rev.* 106 (3), 1105–1136. doi:10.1021/cr050569o
- Vergara-Reyes, H. N., Acosta-Alejandro, M., and Chigo-Anota, E. (2021). Quantum-mechanical assessment of the adsorption of nitric oxide molecules on the magnetic carbon nitride (C₃₆N₂₄)– fullerene. *Struct. Chem.* 32, 1775–1786. doi:10.1007/s11224-021-01736-8
- Yang, H., Song, Y., Zhang, Y., and Chen, H. (2018). Prediction of the electron redundant SinNn fullerenes. *Phys. E* 99, 208–214. doi:10.1016/j.physe.2018.02.010
- Yarovskiy, I., and Goldberg, A. (2005). DFT study of hydrogen adsorption on Al₁₃clusters. *Mol. Simul.* 31 (6-7), 475–481. doi:10.1080/08927020412331337041
- Yilanci, A., Dincer, I., and Ozturk, H. K. (2009). A review on solar-hydrogen/fuel cell hybrid energy systems for stationary applications. *Prog. Energy Combust. Sci.* 35 (3), 231–244. doi:10.1016/j.pecs.2008.07.004
- Zhai, H.-J., Zhao, Y.-F., Li, W.-L., Chen, Q., Bai, H., Hu, H.-S., et al. (2014). Observation of an all-boron fullerene. *Nat. Chem.* 6, 727–731. doi:10.1038/nchem.1999
- Zhang, W. J., Rabiei, S., Bagreev, A., Zhuang, M. S., and Rasouli, F. (2008). Study of NO adsorption on activated carbons. *Appl. Catal. B-Environ.* 83 (1), 63–71. doi:10.1016/j.apcatb.2008.02.003
- Züttel, A., Remhof, A., Borgschulte, A., and Friedrichs, O. (2010). Hydrogen: The future energy carrier. *Philos. Trans. R. Soc. A* 368, 3329–3342. doi:10.1098/rsta.2010.0113